



Precision at the Microscale: Advancing Scientific Discovery with the Dolomite MitoS System

Performance and process optimization of the Dolomite MitoS System for generating a wide size range of water droplets in a FluoSurf carrier phase.

Version: 1.0

Issue Date: Mar-2024

Author: CK/MW



Unchained Labs, LLC., 4747 Willow Road, Pleasanton, CA 94588

E: info@dolomite-microfluidics.com W: dolomite-microfluidics.com

Dolomite is part of Unchained Labs.

1 Introduction

Microfluidic aqueous droplets emerge as a transformative tool with extensive applications across various scientific disciplines, from healthcare to chemistry. Their diminutive size enables unprecedented precision in manipulation and control, facilitating high-throughput experiments with minimal reagent usage. In the realm of biological assays, these droplets revolutionize single-cell analyses by enhancing sensitivity and diminishing sample prerequisites. Moreover, they serve as ideal containers for encapsulating biomolecules or cells, isolating them from external influences and facilitating compartmentalized reactions.

Furthermore, microfluidic aqueous droplets serve as a dynamic foundation for microparticle synthesis. Through precisely controlling droplet formation and manipulation, it's possible to engineer microparticles with specific attributes such as size, shape, and chemical composition. These microparticles find extensive use in biomedicine for applications like targeted drug delivery, where their uniformity and consistency ensure reliable therapeutic effects. In diagnostics, they enhance the precision and specificity of assays for disease detection and monitoring. Moreover, in synthetic chemistry, microfluidic droplets facilitate the creation of intricate microparticle structures, opening new avenues in the development of novel materials and functionalized surfaces. The versatility of microfluidic aqueous droplets thus holds immense promise for propelling advancements in science and technology.

Distinguished by Dolomite's capability to design and fabricate specific glass/quartz chips for a myriad of applications, the Dolomite MitoS System is a unique and generic lab-scale tool for driving innovations in drug discovery, encapsulation, microparticle synthesis, material science, biological research, and diagnostics development. This distinctive feature enables researchers in both academic and industry labs to access an extensive library of chips and flow sensors within the Dolomite Application Packs, guaranteeing optimal performance across diverse experimental conditions through customizable geometries, channel dimensions, and surface chemistries. Whether it is generating monodisperse droplets, encapsulating biomolecules, or producing uniform microparticles, the Dolomite MitoS System stands unparalleled in its versatility and precision, empowering researchers to confidently pursue their scientific goals.

Featuring advanced capabilities such as precise flow control, temperature regulation, and automated operations, the Dolomite MitoS System ensures efficient and reproducible droplet generation. It offers adaptability in modifying flow rates, flow phase ratios, and channel geometries to customize droplet properties according to specific demands. Additionally, it accommodates a wide range of fluids and additives, facilitating the incorporation of diverse components into droplets for various applications, including drug delivery, chemical synthesis, and bioassays. Altogether, the Dolomite MitoS System equips researchers with a powerful platform for exploring and manipulating droplet-based phenomena with unmatched precision and control.

This Application Note concentrates on generating water droplets using a fluorosurfactant carrier phase - FluoSurf - with the Dolomite MitoS System, complemented by two Dolomite Application Packs. This initiative addresses the growing demand for precise and reliable droplet generation techniques across scientific and industrial sectors. By harnessing the capabilities of Dolomite MitoS System, we aim to demonstrate the feasibility and efficacy of employing FluoSurf as a carrier phase for generating water droplets. This approach offers several advantages, including heightened stability, reduced interfacial tension, and enhanced compatibility with hydrophobic substances. Through this application note, we seek to showcase the versatility of the Dolomite MitoS System in facilitating aqueous droplet-based experiments, ultimately contributing to advancements in fields such as pharmaceuticals, biotechnology, and materials science.

2 Dolomite MitoS System Set-up

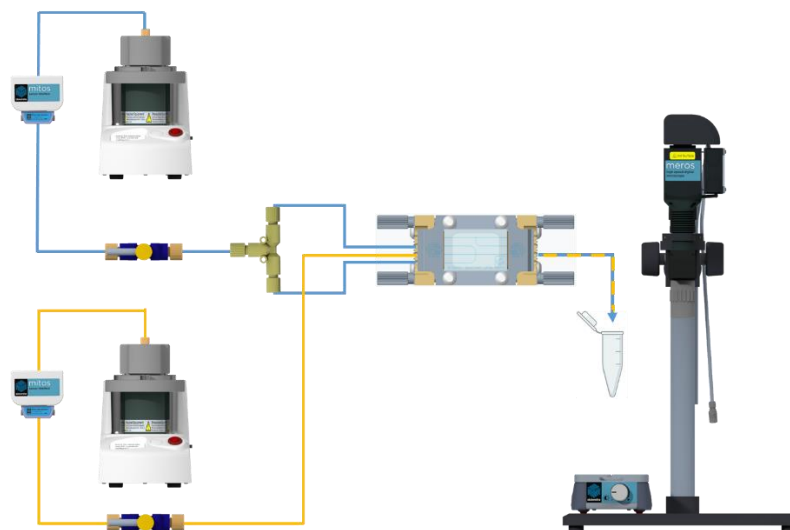


Figure 1 Schematics of the Dolomite MitoS System.

The Dolomite MitoS System (Part number: 3201105) was adeptly utilized for the generation of water-in-oil droplets, employing microfluidic chips with an assortment of junction sizes. The setup outlines as in Figure 1 the assembly of essential components and the fluidic arrangement which includes three precision P-Pumps, ensuring the accurate delivery of fluids. The continuous phase – 2% FluoSurf in Fluoridrop 7500 (part number: 3200808 for a 10 mL pack) – was administered by one pump, while the droplet phase, utilizing molecular biology grade water (Thermo Fisher, part number: J71786.K8), was managed by the second pump. The third pump, provided as an optional component, can be utilized as a flush pump.

This Application Note details the use of two Dolomite Application Packs, containing four specialized chips. Each pack is integrated with corresponding flow rate sensors and 2% FluoSurf in Fluoridrop 7500. The fluidic connections were carefully assembled using tubing kits specifically designed for each pack, encompassing FEP tubing (1.6mm OD, 0.25mm ID), two-way in-line valves for accurate regulation of fluid streams, T-connectors to facilitate fluid branching, and connectors tailored to the specifications of each chip.

- Application Pack: Aqueous Droplets 10 μm - 30 μm (Part number: 32001100) utilized the Small Droplet Chip 14 μm (Fluorophilic).
- Application Pack: Aqueous Droplets 60 μm - 300 μm (Part number: 32001101) was compatible with: Droplet Junction Chip 100 μm (Fluorophilic), Droplet Junction Chip 190 μm (Fluorophilic) and Droplet Junction Chip 275 μm (Fluorophilic).

An array of fluorophilically coated chips featuring various junction sizes were assessed to identify the range of achievable droplet sizes using the Dolomite MitoS System. The 14 μm chip was fitted with a Chip Top Interface and one Linear Connector 4-Way to accommodate its distinctive microfluidic mixing design (refer to Figure 2A), whereas the 100 μm , 190 μm , and 275 μm chips were configured with a Chip Interface H and two Linear Connectors 4-Way (refer to Figure 2B),

Junction imagery was captured for documentation and analysis using the Dolomite Imaging Pack equipped with High-Speed Microscope and Camera (Part number: 3201107).

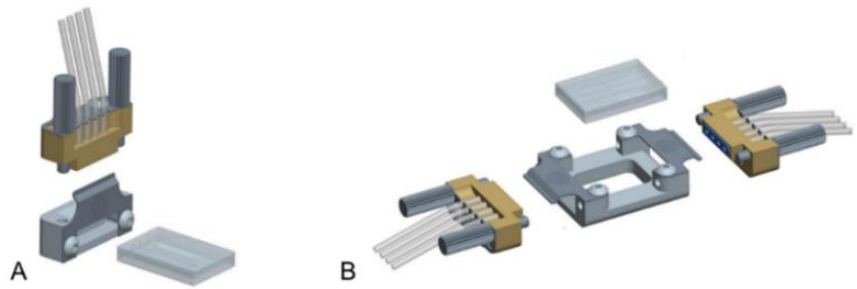


Figure 2 Chip Top Interface and one Linear Connector 4-Way for Application Pack: Aqueous Droplets 10 μm - 30 μm in A; Chip Interface H and two Linear Connector 4-Way for Application Pack: Aqueous Droplets 60 μm - 300 μm in B.

3 Results and Discussion

3.1 Droplet Size against Chip Junction Size

The Dolomite Mitos System is demonstrated to proficiently employ microfluidic methodologies for the production of monodisperse emulsions. A detailed investigation into microfluidic droplet generation, facilitated by droplet junction chips with varying dimensions, has elucidated a clear correlation between the size of the junction and the diameter of the resulting droplets, as depicted in Figure 3. It was discernibly observed that chips with smaller junction dimensions, notably the 14 μm chip, were responsible for generating droplets within the diminutive range of 10 μm to 30 μm . In contrast, chips with larger junction sizes, including those of 100 μm , 190 μm , and 275 μm , progressively produced larger droplets, with diameters extending from 65 μm to 310 μm . Such empirical evidence firmly establishes the pivotal role of junction size in modulating droplet dimensions within microfluidic platforms, offering critical insights for the nuanced optimization and design of droplet-centric assays and devices. The findings affirm the significant role of chip geometry in the precision of droplet sizing, establishing a direct correlation between a chip's dimensions and its capacity for droplet formation. Therefore, the careful selection of chip size becomes a key strategy in microfluidic droplet generation, enabling the customization of droplet characteristics to suit a wide array of application needs.

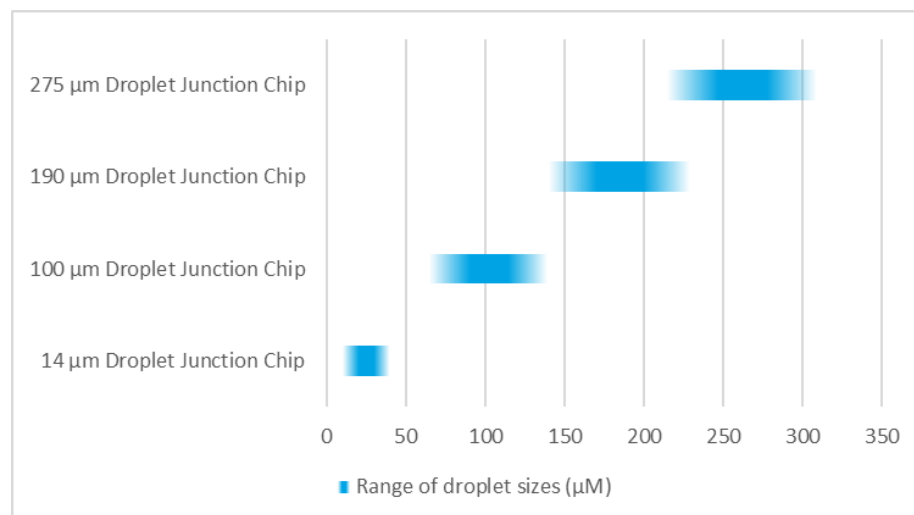


Figure 3 Droplet size range in μm .

Figure 4 provides a detailed graphical representation of the aqueous droplet sizes achieved using different chip geometries, showing the variance across chips with junction dimensions of 14 μm , 100 μm , 190 μm , and 275 μm . This figure effectively distills the qualitative assessment of droplet dimensions across the range of tested chip sizes, unequivocally starting the direct link between the physical dimensions of the chip junctions and the diameters of the droplets produced. The visual summary presented in Figure 4 is crucial for understanding the scalability and adaptability of droplet formation within microfluidic systems, facilitating precise control over droplet size for a multitude of applications in science and industry.

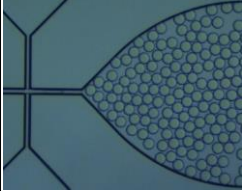
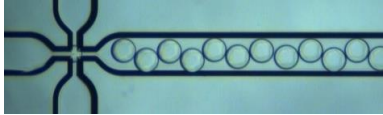
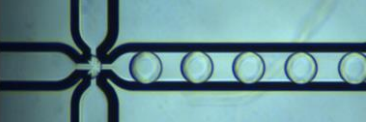
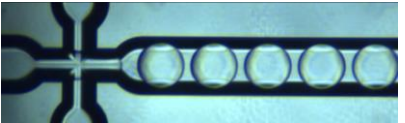
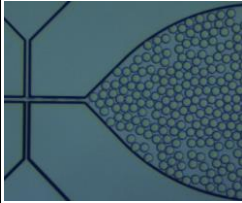
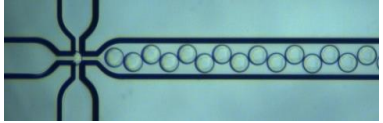
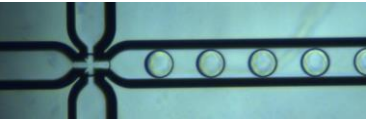
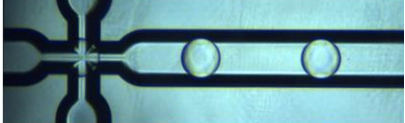
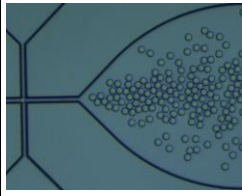
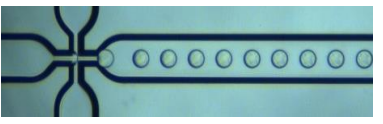
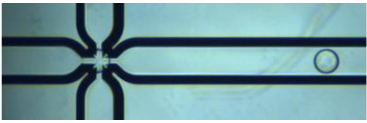

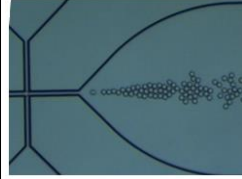
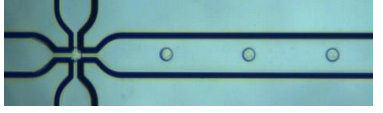
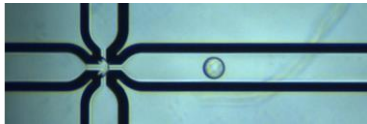
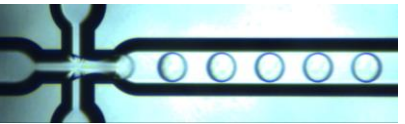
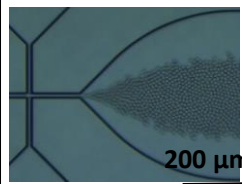


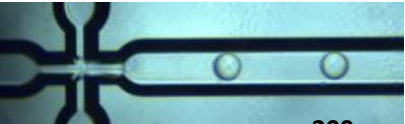
Size (µm)	14 µm Droplet Junction Chip	Size (µm)	100 µm Droplet Junction Chip	Size (µm)	190 µm Droplet Junction Chip	Size (µm)	275 µm Droplet Junction Chip
30		140		233		310	
24		123		210		279	
20		97		186		250	
15		80		152		237	
10		65		139		214	

Figure 4 Aqueous microdroplet generated in different droplet junction chips using molecular biology grade water as droplet phase and 2% FluoSurf in Fluoridrop 7500 as carrier phase. The size of droplet is normalised against the volume calculated to achieve spherical droplet diameter. Scale bar = 200 µm.

3.2 Droplet Volume and Diameter Calculations

Droplet volume is typically determined by assuming a spherical shape for the droplet, as illustrated in Figures 4. However, if the diameter of the droplet observed within a microchannel exceeds the channel's depth, the droplet will assume a flattened cylindrical shape, as depicted below in Figure 5. The formula for calculating the volume of such a cylinder is presented below. Within this application note, the droplet size is normalized based on the computed volume, accounting for the droplet's deformation into a squashed shape post-junction within the chip.

Equations Used

For Spherical Droplet

Volume of Droplet

Droplet $D <$ Channel Depth

$$V = \frac{4}{3}\pi r^3$$

For Squashed Cylinder

Volume of Cylinder

$$V_c = \pi d \left(r - \frac{d}{2} \right)^2$$

Distance to Centroid

$$c = r - \frac{d}{2} + \frac{4}{3} \frac{\left(\frac{d}{2} \right)}{\pi}$$

Area of Semicircle

$$A_s = \pi \frac{d^2}{8}$$

Volume of Semicircular Ring

$$V_s = 2\pi A_s c$$

Total Droplet Volume

$$V_t = V_c + V_s$$

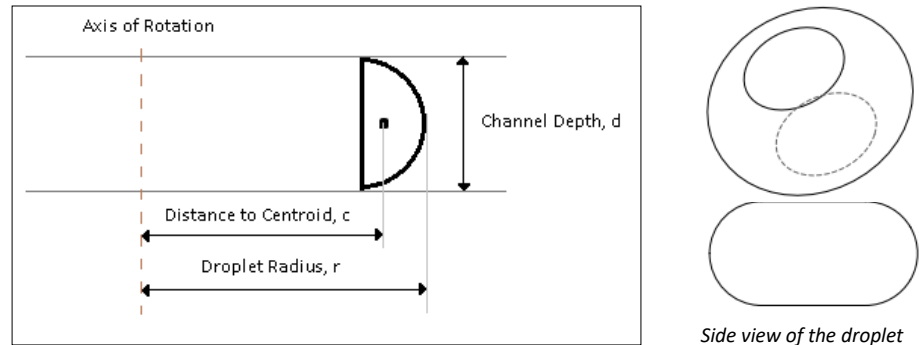


Figure 5 Shape of a droplet within the chip.

3.3 Droplet Size against Flow Rate and Flow Rate Ratio

Droplet dimensions are intricately influenced by the flow rates of both the droplet and carrier fluids, which, in this set of experiments, correspond to the aqueous/water and oil phases, respectively. When the flow rate of the droplet phase is held constant, an increase in the carrier fluid's flow rate results in the formation of smaller droplets. Simultaneously, chip size significantly impacts droplet dimensions, with smaller chips tending to produce smaller droplets. Additionally, the internal pressure of the microfluidic system plays a pivotal role in the spacing between droplets, where decreased spacing correlates with a higher likelihood of droplet coalescence. These findings emphasize the sophisticated relationship among flow rates, system pressures, and chip sizes in dictating both droplet size and their spatial distribution. Achieving a fine balance between these variables is crucial for controlling droplet size and reducing

coalescence, imperative for applications requiring precise droplet manipulation and stability.

A systematic approach prompted the detailed examination of the 100 μm droplet junction chip, selected after an exhaustive analysis of droplet junction chips with dimensions of 14 μm , 100 μm , 190 μm , and 275 μm . This choice was predicated on the ability of the 100 μm droplet junction chip to facilitate the creation of droplets spanning a wide range of sizes, making it an ideal candidate for investigating how modifications in flow rate influence droplet formation and characteristics.

The goal of this study is to delineate the operating conditions conducive to stable droplet production. Experimental imagery (referenced as Figure 6) captures the distinct flow regimes encountered across various combinations of flow rates. A total of four unique flow regimes were identified, each illustrating the nuanced effects of flow rate adjustments on droplet generation.

- **Dripping regime** – Monodisperse droplets are achieved. The monodispersity can be quantified in terms of coefficient of variation, which is expected to be within 5%. This is a desirable operating zone.
- **Jetting regime** – This occurs at higher flow rates and can result in monodispersed droplets but can also give polydispersed droplets. At very high flow rates annular flow can occur with no droplet formation.
- **Chaotic** – In this zone, the cumulative flow rates are excessively high. Varying the flow ratios fails to cause droplet pinchoff and as a result, the droplet formation fails. This is undesirable.
- **Backflow** – This is characterised by the oil stream flowing back into the water feed channel. To avoid backflow the resistance of the flow resistor on the water input stream should be increased.

Figure 7 displays a logarithmically scaled correlation between oil and aqueous phase flow rates, indicating a positive trend wherein an increase in the oil phase flow rate is generally accompanied by a higher aqueous phase flow rate. The data exhibit clustering at specific oil flow rates, suggesting distinct operational regimes that influence the system's droplet production stability. These findings are instrumental for understanding and controlling microfluidic system behaviour to maintain optimal droplet generation performance.

The data depicted in Figure 8 highlights the impact of the oil-to-aqueous phase flow rate ratio on the size of the generated droplets at maximum throughput conditions. This ratio, expressed as the oil phase flow rate divided by the aqueous phase flow rate, inversely correlates with droplet size. As observed, when the ratio is low, droplets are comparatively larger, and a marked decrease in droplet size is noted with the increase in the ratio. This inverse relationship demonstrates a steep decrease in droplet size as the ratio increases from 1 to approximately 2. As the ratio continues to rise towards 6, the rate of decrease in droplet size diminishes, suggesting a tapering effect that could indicate an approach toward a minimum droplet size achievable under the given system conditions for a 100 μm droplet junction chip. The trend presented here underscores the delicate balance required in modulating flow rates for the precise control of droplet size, which is essential for the fine-tuning of droplet-based systems for specific microfluidic applications. The dotted trend line forecasts a continuation of this pattern, albeit at a reduced rate of change, implying that further manipulation of the flow rate ratio may only yield marginal reductions in droplet size beyond a certain threshold.






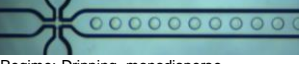









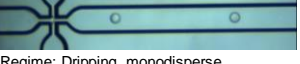
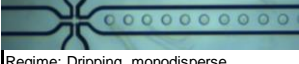
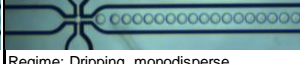
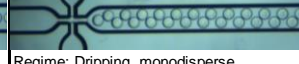


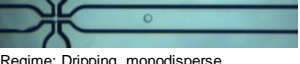
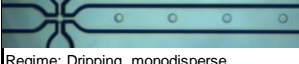
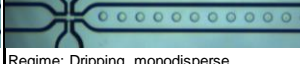

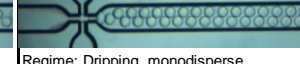
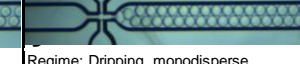
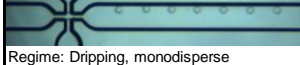
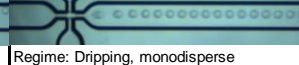
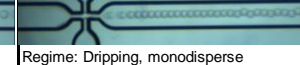
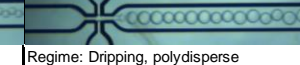

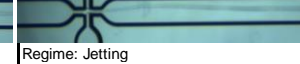
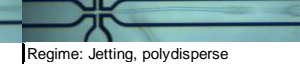
		Aqueous Flow Rate ($\mu\text{L}/\text{min}$)					
		1	3	10	30	60	100
Oil Flow Rate ($\mu\text{L}/\text{min}$)	1	 Regime: Dripping, monodisperse Rate: 4 dps Size: 193.2 μm	 Regime: Dripping, monodisperse Rate: Size:				
	3	 Regime: Dripping, monodisperse Rate: 12 dps Size: 140 μm	 Regime: Dripping, monodisperse Rate: 18 dps Size: 172.9 μm	 Regime: Dripping, monodisperse Rate: Size:		Chaotic	
	10	 Regime: Dripping, monodisperse Rate: 24 dps Size: 110.4 μm	 Regime: Dripping, monodisperse Rate: 52 dps Size: 122.6 μm	 Regime: Dripping, monodisperse Rate: 133 dps Size: 133.8 μm	 Regime: Dripping, monodisperse Rate: Size:		
	30	 Regime: Dripping, monodisperse Rate: 44 dps Size: 89.9 μm	 Regime: Dripping, monodisperse Rate: 104 dps Size: 97.1 μm	 Regime: Dripping, monodisperse Rate: 236 dps Size: 110.6 μm	 Regime: Dripping, monodisperse Rate: 486 dps Size: 125.2 μm	 Regime: Dripping, monodisperse Rate: 882 dps Size: 129.4 μm	 Regime: Dripping, chaotic
	60	 Regime: Dripping, monodisperse Rate: 45 dps Size: 89.4 μm	 Regime: Dripping, monodisperse Rate: 120 dps Size: 92.5 μm	 Regime: Dripping, monodisperse Rate: 394 dps Size: 93.1 μm	 Regime: Dripping, monodisperse Rate: 844 dps Size: 104.2 μm	 Regime: Dripping, monodisperse Rate: 1303 dps Size: 113.6 μm	 Regime: Dripping, monodisperse Rate: 1958 dps Size: 117.6 μm
	100	 Regime: Dripping, monodisperse Rate: 77 dps Size: 74.5 μm	 Regime: Dripping, monodisperse Rate: 185 dps Size: 80.2 μm	 Regime: Dripping, monodisperse Rate: 504 dps Size: 85.8 μm	 Regime: Dripping, monodisperse Rate: 1063 dps Size: 95.6 μm	 Regime: Dripping, monodisperse Rate: 1860 dps Size: 100.9 μm	 Regime: Dripping, monodisperse Rate: 2970 dps Size: 102.4 μm
	300			 Regime: Dripping, monodisperse Rate: 1460 dps Size: 60.2 μm	 Regime: Dripping, monodisperse Rate: 3400 dps Size: 65.5 μm	 Regime: Dripping, monodisperse Rate: 6266 dps Size: 67.3 μm	 Regime: Dripping, polydisperse Rate: Size:
	1000		Backflow		 Regime: Jetting Rate: Size:	 Regime: Jetting Rate: Size:	 Regime: Jetting, polydisperse Rate: Size:

Figure 6 Chart showing flow regimes at varied flow rates for 100 μm droplet junction chip using molecular biology grade water as droplet phase and 2% FluoSurf in Fluoridrop 7500 as carrier phase. The size of droplet is normalised against the volume calculated to achieve spherical droplet diameter.

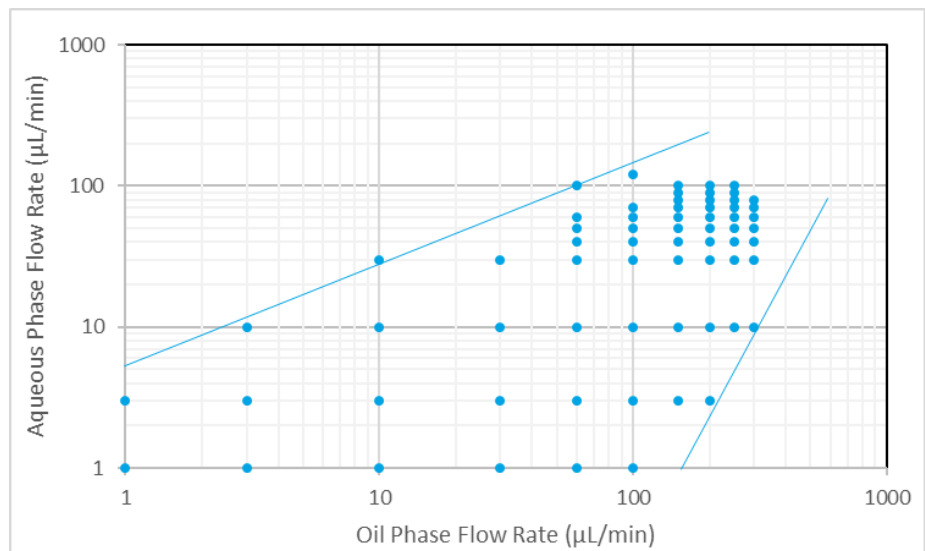


Figure 7 Aqueous flow rate vs oil flow rate for 100 μm junction chip using molecular biology grade water as droplet phase and 2% FluoSurf in Fluoridrop 7500 as carrier phase.

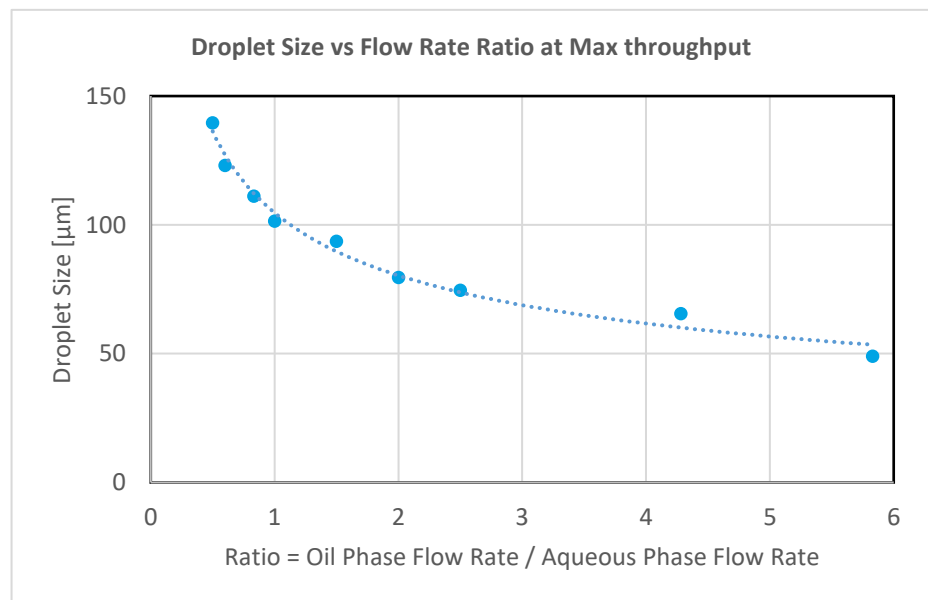


Figure 8 Droplet size vs flow rate ratio at max throughput for 100 μm junction chip using molecular biology grade water as droplet phase and 2% FluoSurf in Fluoridrop 7500 as carrier phase.

3.4 Flow Rate Calculation

The fluidic layout can normally be represented schematically as shown in the diagram below (as Figure 9) where W is the water droplet stream and O is the oil carrier fluid. This assumes that the flow resistance after the droplet junction, R_d , is low relative to the flow resistance of the two input streams R_w and R_o .

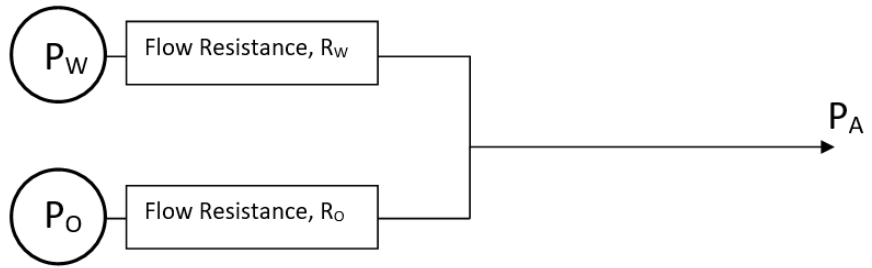


Figure 9 Flow resistance for water and oil in the diagram.

The flow rate in each feed stream can be estimated using the following two equations:

$$Q_W = \frac{P_W}{R_W \times \mu_W}, \quad Q_O = \frac{P_O}{R_O \times \mu_O}$$

Q = flow rate

P = pressure in P-Pump

μ = viscosity

R = flow resistance

The Microfluidic Calculator on www.dolomite-microfluidics.com can be used to estimate flow rates using the equation shown above.

If R_j is high relative to R_x and R_y then it is necessary to first calculate the pressure at the droplet junction to get an accurate estimate of all the flow rates in the system.

The schematic below in Figure 10 shows R_j and the equation can be used to estimate the pressure at the junction, P_j . The equation assumes that the viscosity of the output stream is equal to the viscosity of the carrier fluid. This is generally a good approximation if the carrier flow rate is higher than the droplet flow rate.

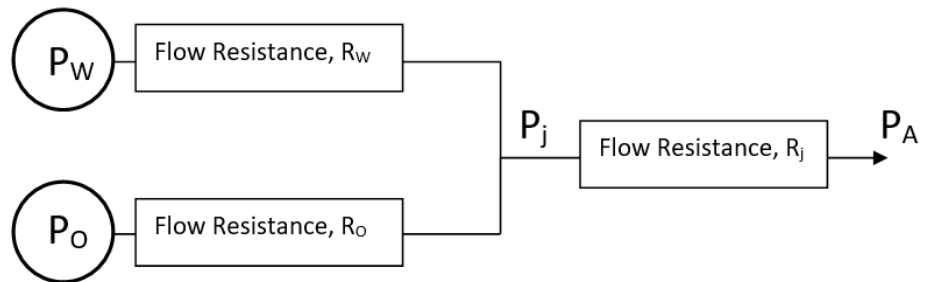


Figure 10 Flow resistance at the junction of the chip.

$$P_j = \frac{P_W \cdot W + P_O \cdot O}{J + W + O}$$

Where:

$$W = \frac{1}{R_W \times \mu_W}, \quad O = \frac{1}{R_O \times \mu_O}, \quad J = \frac{1}{R_j \times \mu_O}$$

R_w = flow resistance of the water input channel

R_o = flow resistance of the oil input channel

R_j = flow resistance of the channel after the junction

μ_w = viscosity of water

μ_o = viscosity of oil

P_j = pressure at the junction

P_w = P-Pump pressure on water

P_o = P-Pump pressure on oil

The flow rates can then be calculated as follows:

$$Q_w = (P_w - P_j) \cdot W, \quad Q_o = (P_o - P_j) \cdot O$$

These equations are useful for predicting backflow scenarios for a P-Pump set-up.

4 Conclusion

In conclusion, the Dolomite MitoS System has been demonstrated to proficiently leverage microfluidic technologies for the production of uniform and monodisperse emulsions. Our results have conclusively established that the size of the droplet junction chips is a significant factor in determining the size of the resulting droplets, with smaller chips generating smaller droplets and vice versa. This insight is fundamental for the advancement of droplet-based assays and devices, enabling precise control over droplet size which is critical for a multitude of applications across various scientific fields. The data also suggest the presence of distinct operational flow regimes, which have implications for the stability and uniformity of droplet production. Our observations on the relationship between droplet size and flow rate ratios offer a predictive understanding that can be harnessed to fine-tune microfluidic systems for specific experimental needs. This study's findings provide a solid foundation for further research and optimization in the field of microfluidics, with the potential to revolutionize applications in drug discovery, diagnostics, and materials science, among others. The insights gained here contribute significantly to the expanding capabilities of the Dolomite MitoS System, enhancing its standing as an indispensable tool for researchers and developers in the cutting-edge arena of microfluidics.